Int J Mech Mater Des (2010) 6:163–174
DOI 10.1007/s10999-010-9124-4

An electromechanical higher order model for piezoelectric functionally graded plates

S. M. Shiyekar · Tarun Kant

Received: 19 March 2010 / Accepted: 31 March 2010 / Published online: 23 April 2010

Abstract Bidirectional flexure analysis of functionally graded (FG) plate integrated with piezoelectric fiber reinforced composites (PFRC) is presented in this paper. A higher order shear and normal deformation theory (HOSNT12) is used to analyze such hybrid or smart FG plate subjected to electromechanical loading. The displacement function of the present model is approximated as Taylor's series in the thickness coordinate, while the electro-static potential is approximated as layer wise linear through the thickness of the PFRC layer. The equations of equilibrium are obtained using principle of minimum potential energy and solution is by Navier's technique. Elastic constants are varying exponentially along thickness (z axis) for FG material while Poisson's ratio is kept constant. PFRC actuator attached either at top or bottom of FG plate and analyzed under mechanical and coupled mechanical and electrical loading. Comparison of present HOSNT12 is made with exact and finite element method (FEM).

Keywords Higher order theory · Piezoelectric fiber reinforced composites · Functionally Graded

S. M. Shiyekar (✉)
Department of Civil Engineering, Sinhgad College of Engineering, Vadgaon (Bk), Pune 411 041, India
e-mail: smshiyekar.scoe@sinhgad.edu

T. Kant
Department of Civil Engineering, Indian Institute of Technology Bombay, Powai 400 076, India
e-mail: tkant@civil.iitb.ac.in

1 Introduction

Piezoelectric materials transform elastic field into the electric field and converse behavior leads many researchers to study their controlling capabilities applicable to structures like plates and shells. Such structures are called as smart, intelligent, adaptive as well as hybrid structures. In conventional composites failure occurs at interface due to abrupt change in material properties. Elastic properties are varying smoothly across the thickness of the FG material and hence failure due to de lamination is avoided.

Piezoelectric materials show coupling phenomenon between elastic and electric fields. Tiersten and Mindlin (1962) initiated work on piezoelectric plates. Further Tiersten (1969) contributed this work by exploring the governing equations of linear piezoelectric continuum by analyzing vibrations of a single piezoelectric layer.

Monolithic piezoelectric materials exhibit very low stress/strain coefficients and hence low controlling capabilities. Smith and Auld (1991) presented micromechanical analysis of vertically reinforced piezoelectric composites with slight increase in the stress/strain piezoelectric coefficients.

Mallik and Ray (2003) proposed the concept of unidirectional piezoelectric fiber reinforced composite (PFRC) materials and presented their effective elastic and piezoelectric properties. Piezoelectric stress/strain coefficients are improved considerably as compared to monolithic piezoelectric materials. Vertically

reinforced piezoelectric composites are not suitable for the bending mode actuation (Mallik and Ray 2003).

Many investigators studied hybrid composite laminates using various plate theories. Kapuria and Dumir (2000) presented coupled first-order shear deformation theory for hybrid laminated plates subjected to thermoelectrical loading. Elasticity solutions always serve as benchmark for other approximate solutions. Ray et al. (1993) developed three-dimensional (3D) elasticity solutions for intelligent plate simply supported and perfectly bonded with distributed Polyvinylidene Fluoride (PVDF) piezoelectric layers at top and bottom and presented static displacement control for different span to depth ratios. Heyliger (1994) obtained exact solution for an unsymmetric cross ply composite laminate attached with PZT-4 layers of piezoelectric material at upper and lower surfaces. The 3D solution methodology used by Ray and Heyliger is the same as the work of Pagano (1970) for laminated composite plates. Later Heyliger (1997) provided the 3D exact solution for single and two layers of piezoelectric materials. Vel and Batra (2000) used Eshelby-Stroh formulation to obtained 3D elasticity solution to analyze multilayered piezoelectric plate for arbitrary boundary conditions. Batra and Vel (2001) presented exact thermo elastic solutions for FG plates, while Sankar (2001) presented 3D exact solutions for functionally graded beams under mechanical pressure. Ray and Sachade (2006a, b) reported 3D elasticity solution and FEM for FG plate attached with PFRC actuator. Reddy and Cheng (2001) also presented elasticity solutions for smart FG plate.

Higher order shear deformation theories (HOST) incorporate transverse shear and normal deformation by expanding the primary displacement fields. Initially Kant (1982) developed complete set of variationally consistent governing equations of equilibrium and presented first FE model based on HOST (Kant et al. 1982). Pandya and Kant (1987, 1988) and Kant and Manjunatha (1988, 1994) extended the HOST for unsymmetric laminates. Further Kant and Swaminathan (2002) presented a refined higher order theory and discussed analytical solution for sandwiches and laminates. Reddy (1984) presented a simple third order theory for laminates maintaining zero shear stress conditions at boundaries of the thickness dimension.

In this paper, a higher order shear and normal deformation theory (HOSNT12) is used to model the elastic displacements of FG plate whereas; electric potential in the PFRC actuator layer is modeled as piece wise linear.

2 Formulation

Consider bidirectional flexure of functionally graded (FG) plate. At $x = 0, a$ and at $y = 0, b$ the FG plate is simply supported and attached with distributed PFRC actuator of thickness t_p at top or bottom as shown in the Fig. 1. Span of the hybrid FG plate is a along x axis and b along y axis in Cartesian coordinate system. Thickness of FG plate is h along z axis and located at $-h/2$ and $+h/2$ from bottom and top of FG plate, respectively. Electrostatic potential is applied at top of PFRC actuator ($h/2 + t_p$) and FG plate is electrically grounded at $z = +h/2$.

Displacement components $u(x,y,z)$, $v(x,y,z)$ and $w(x,y,z)$ at any point in the plate are expanded in a

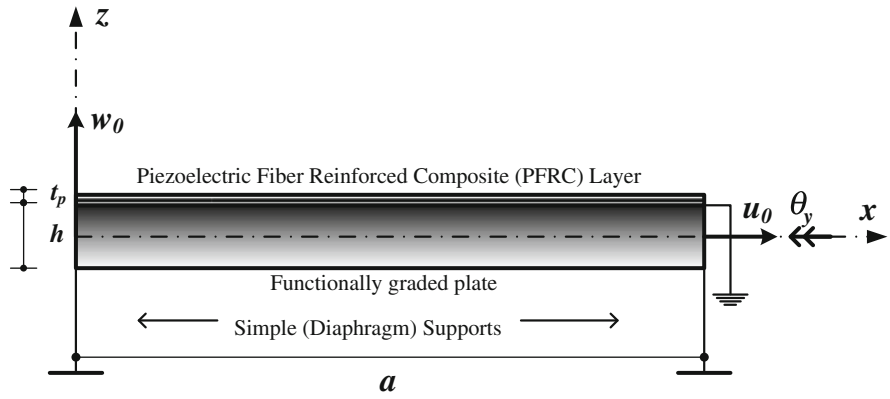

Fig. 1 Geometry of Functionally Graded (FG) simply (diaphragm) supported along all edges plate attached with PFRC actuator

Taylor's series to approximate the three-dimensional (3D) elasticity problem as a two-dimensional (2D) plate problem. The assumed displacement field of present higher order shear and normal deformation model is in the following form:

Model HOSNT12: (Kant and Swaminathan 2002)

$$\begin{aligned} u(x,y,z) &= u_0(x,y) + z\theta_x(x,y) + z^2 u_0^*(x,y) + z^3\theta_x^*(x,y) \\ v(x,y,z) &= v_0(x,y) + z\theta_y(x,y) + z^2 v_0^*(x,y) + z^3\theta_y^*(x,y) \\ w(x,y,z) &= w_0(x,y) + z\theta_z(x,y) + z^2 w_0^*(x,y) + z^3\theta_z^*(x,y) \end{aligned} \tag{1}$$

where the parameters u_0, v_0 are in-plane displacements and w_0 is transverse displacement at any point (x, y) on the middle plane of the plate. θ_x & θ_y are the rotations of the normal to the mid-plane about y and x axes, respectively. Other parameters such as $u_0^*, \theta_x^*, v_0^*, \theta_y^*, w_0^*, \theta_z^*$ are the corresponding higher order terms in the Taylor series expansion at mid-plane.

Strain displacement relationship as per classical theory of elasticity is written in Eq. 2 as

$$\begin{Bmatrix} \varepsilon_x \\ \varepsilon_y \\ \varepsilon_z \\ \gamma_{xy} \\ \gamma_{yz} \\ \gamma_{xz} \end{Bmatrix} = \left\{ \frac{\partial u}{\partial x} \;\; \frac{\partial v}{\partial y} \;\; \frac{\partial w}{\partial z} \;\; \frac{\partial u}{\partial y} + \frac{\partial v}{\partial x} \;\; \frac{\partial v}{\partial z} + \frac{\partial w}{\partial y} \;\; \frac{\partial u}{\partial z} + \frac{\partial w}{\partial x} \right\}^t \tag{2}$$

Tiersten (1969) presented linear constitutive equation which couples the elastic and electric field for a single piezoelectric layer as

$$\begin{aligned} \{\sigma\} &= [C]\{\varepsilon\} - [e]\{E\}^L \\ \{D\} &= [e]^t\{\varepsilon\} + [\eta]\{E\}^L \end{aligned} \tag{3}$$

The electric field intensity vector E related to electrostatic potential $\xi(x,y,z)$ in the Lth layer is given by

$$E_x^L = -\frac{\partial \xi(x,y,z)^L}{\partial x}, \quad E_y^L = -\frac{\partial \xi(x,y,z)^L}{\partial y}, \quad E_z^L = -\frac{\partial \xi(x,y,z)^L}{\partial z}$$

where σ, Q, ε, e, E, D and η are, stress vector, elastic constant matrix, strain vector, piezoelectric constant matrix, electric field intensity vector, electric displacement vector and dielectric constant matrix, respectively. Effective piezoelectric constant matrix e and dielectric matrix η for PFRC layer aligned at zero angle with respect to x-axis is given by Mallik and Ray (2003) as

$$[e] = \begin{bmatrix} 0 & 0 & e_{31} \\ 0 & 0 & e_{32} \\ 0 & 0 & e_{33} \\ 0 & 0 & 0 \\ 0 & e_{24} & 0 \\ e_{15} & 0 & 0 \end{bmatrix}, \quad [\eta] = \begin{bmatrix} \eta_{11} & 0 & 0 \\ 0 & \eta_{22} & 0 \\ 0 & 0 & \eta_{33} \end{bmatrix} \tag{5}$$

The first set of Eq. 3 is divided in two components of stresses. One is elastic stress component (*es*) and other is piezoelectric stress component (*pz*).

First set of Eq. 3 is written as $\{\sigma\} = \{\sigma\}^{es} - \{\sigma\}^{pz}$ where

$$\{\sigma\}^{es} = \begin{bmatrix} C_{11} & C_{12} & C_{13} & 0 & 0 & 0 \\ C_{12} & C_{22} & C_{23} & 0 & 0 & 0 \\ C_{13} & C_{23} & C_{33} & 0 & 0 & 0 \\ 0 & 0 & 0 & C_{44} & 0 & 0 \\ 0 & 0 & 0 & 0 & C_{55} & 0 \\ 0 & 0 & 0 & 0 & 0 & C_{66} \end{bmatrix}^L \begin{Bmatrix} \varepsilon_x \\ \varepsilon_y \\ \varepsilon_z \\ \gamma_{xy} \\ \gamma_{yz} \\ \gamma_{xz} \end{Bmatrix},$$

$$\{\sigma\}^{pz} = \begin{bmatrix} 0 & 0 & e_{31} \\ 0 & 0 & e_{32} \\ 0 & 0 & e_{33} \\ 0 & 0 & 0 \\ 0 & e_{24} & 0 \\ e_{15} & 0 & 0 \end{bmatrix}^L \begin{Bmatrix} -\frac{\partial \xi(x,y,z)}{\partial x} \\ -\frac{\partial \xi(x,y,z)}{\partial y} \\ -\frac{\partial \xi(x,y,z)}{\partial z} \end{Bmatrix}^L \tag{6}$$

and C_{ij} are elastic constants of FG plate and defined as per isotropic layer.

$$\begin{aligned} C_{11} = C_{22} = C_{33} &= \frac{(1-v)E(z)}{(1+v)(1-2v)}; \\ C_{12} = C_{13} = C_{23} &= \frac{vE(z)}{(1+v)(1-2v)}; \\ C_{44} = C_{55} = C_{66} &= \frac{E(z)}{2(1+v)} = G. \end{aligned} \tag{7}$$

Young's modulus of FG material is a function of z coordinate and governed by exponential law (Sankar 2001), where as Poisson's ratio is kept constant.

$$E(z) = E_0 e^{\lambda(z+h/2)} \tag{8}$$

where E_0 is Young's modulus of FG material at bottom and λ is a non-homogeneous parameter of the FG material across the thickness.

Stress resultants are also defined as elastic and piezoelectric stress resultants.

Elastic stress resultants $[Q, S, M, N]^{es}$

$$\left[Q_x^{es}, Q_y^{es} | Q_x^{es^*}, Q_y^{es^*}\right] = \sum_{L=1}^{n} \int_{-h/2}^{+h/2} \left\{\tau_{xz}^{es}, \tau_{yz}^{es}\right\}\left[1|z^2\right]dz, \left[S_x^{es}, S_y^{es} | S_x^{es^*}, S_y^{es^*}\right]$$

$$= \sum_{L=1}^{n} \int_{-h/2}^{+h/2} \left\{\tau_{xz}^{es}, \tau_{yz}^{es}\right\}\left[z|z^3\right]dz$$

$$\left[M_x^{es}, M_y^{es}, M_{xy}^{es} | M_x^{es^*}, M_y^{es^*}, M_{xy}^{es^*}\right] = \sum_{L=1}^{n} \int_{-h/2}^{+h/2} \left\{\sigma_x^{es}, \sigma_y^{es}, \tau_{xy}^{es}\right\}\left[z|z^3\right]dz, M_z^{es}$$

$$= \sum_{L=1}^{n} \int_{-h/2}^{+h/2} \sigma_z^e dz,$$

$$\left[N_x^{es}, N_y^{es}, N_z^{es}, N_{xy}^{es} | N_x^{es^*}, N_y^{es^*}, N_z^{es^*}, N_{xy}^{es^*}\right] = \sum_{L=1}^{n} \int_{-h/2}^{+h/2} \left\{\sigma_x^{es}, \sigma_y^{es}, \sigma_z^{es}, \tau_{xy}^{es}\right\}\left[1|z^2\right]dz. \quad (9)$$

Piezoelectric stress resultants $[Q, S, M, N]^{pz}$

$$\left[Q_x^{pz}, Q_y^{pz} | Q_x^{pz^*}, Q_y^{pz^*}\right] = \int_{+h/2}^{h/2+tp} \left\{\tau_{xz}^{pz}, \tau_{yz}^{pz}\right\}\left[1|z^2\right]dz, \left[S_x^{pz}, S_y^{pz} | S_x^{pz^*}, S_y^{pz^*}\right]$$

$$= \int_{+h/2}^{h/2+tp} \left\{\tau_{xz}^{pz}, \tau_{yz}^{pz}\right\}\left[z|z^3\right]dz$$

$$\left[M_x^{pz}, M_y^{pz}, M_{xy}^{pz} | M_x^{pz^*}, M_y^{pz^*}, M_{xy}^{pz^*}\right] = \int_{+h/2}^{h/2+tp} \left\{\sigma_x^{pz}, \sigma_y^{pz}, \tau_{xy}^{pz}\right\}\left[z|z^3\right]dz, M_z^{pz} = \int_{+h/2}^{h/2+tp} \sigma_z^{pz} dz,$$

$$\left[N_x^{pz}, N_y^{pz}, N_z^{pz}, N_{xy}^{pz} | N_x^{pz^*}, N_y^{pz^*}, N_z^{pz^*}, N_{xy}^{pz^*}\right] = \int_{+h/2}^{h/2+tp} \left\{\sigma_x^{pz}, \sigma_y^{pz}, \sigma_z^{pz}, \tau_{xy}^{pz}\right\}\left[1|z^2\right]dz. \quad (10)$$

Total stress resultants (pz): Total stress resultants $[Q, S, M, N]$ are algebraic sum of elastic and piezoelectric stress resultants.

$$[Q, S, M, N] = [Q, S, M, N]^{es} + [Q, S, M, N]^{pz} \quad (11)$$

Governing equations of equilibrium.

Using principal of minimum potential energy, the equations of equilibrium are obtained as

$$\begin{aligned}
\delta u_0 &: \frac{\partial N_x}{\partial x} + \frac{\partial N_{xy}}{\partial y} = 0 \quad & \delta u_0^* &: \frac{\partial N_x^*}{\partial x} + \frac{\partial N_{xy}^*}{\partial y} - 2S_x = 0 \\
\delta v_0 &: \frac{\partial N_y}{\partial y} + \frac{\partial N_{xy}}{\partial x} = 0 \quad & \delta v_0^* &: \frac{\partial N_y^*}{\partial y} + \frac{\partial N_{xy}^*}{\partial x} - 2S_y = 0 \\
\delta w_0 &: \frac{\partial Q_x}{\partial x} + \frac{\partial Q_y}{\partial y} + (q_z^+) = 0 \quad & \delta w_0^* &: \frac{\partial Q_x^*}{\partial x} + \frac{\partial Q_y^*}{\partial y} - 2M_z^* + \frac{h^2}{4}(q_z^+) = 0 \\
\delta \theta_x &: \frac{\partial M_x}{\partial x} + \frac{\partial M_{xy}}{\partial y} - Q_x = 0 \quad & \delta \theta_x^* &: \frac{\partial M_x^*}{\partial x} + \frac{\partial M_{xy}^*}{\partial y} - 3Q_x^* = 0 \\
\delta \theta_y &: \frac{\partial M_y}{\partial y} + \frac{\partial M_{xy}}{\partial x} - Q_y = 0 \quad & \delta \theta_y^* &: \frac{\partial M_y^*}{\partial y} + \frac{\partial M_{xy}^*}{\partial x} - 3Q_y^* = 0 \\
\delta \theta_z &: \frac{\partial S_x}{\partial x} + \frac{\partial S_y}{\partial y} - N_z + \frac{h}{2}(q_z^+) = 0 \quad & \delta \theta_z^* &: \frac{\partial S_x}{\partial x} + \frac{\partial S_y}{\partial y} - 3N_z^* + \frac{h^3}{8}(q_z^+) = 0
\end{aligned} \quad (12)$$

Total stress resultants are the addition of elastic and piezoelectric stress resultants.

Following are the mechanical boundary conditions used for simply supported plate

$$\begin{aligned}
&\text{At edges } x = 0 \text{ and } x = a:\\
&v_0 = 0,\ w_0 = 0,\ \theta_y = 0,\ \theta_z = 0,\\
&\quad M_x = 0,\ N_x = 0,\ v_0^* = 0,\ w_0^* = 0,\\
&\quad \theta_y^* = 0,\ \theta_z^* = 0,\ M_x^* = 0,\ N_x^* = 0.\\
&\text{At edges } y = 0 \text{ and } y = b:\\
&u_0 = 0,\ w_0 = 0,\ \theta_x = 0,\ \theta_z = 0,\\
&\quad M_y = 0,\ N_y = 0,\ u_0^* = 0,\ w_0^* = 0,\\
&\quad \theta_x^* = 0,\ \theta_z^* = 0,\ M_y^* = 0,\ N_y^* = 0.
\end{aligned} \tag{13}$$

Navier's solution procedure is adopted to find the solution of displacement variables, satisfying the above boundary conditions and is expressed as follows:

$$\begin{aligned}
u_0 &= \sum_{m=1}^{\infty}\sum_{n=1}^{\infty} u_{0_{mn}} \cos\left(\frac{m\pi x}{a}\right) \sin\left(\frac{n\pi y}{b}\right) & u_0^* &= \sum_{m=1}^{\infty}\sum_{n=1}^{\infty} u_{0_{mn}}^* \cos\left(\frac{m\pi x}{a}\right) \sin\left(\frac{n\pi y}{b}\right)\\
v_0 &= \sum_{m=1}^{\infty}\sum_{n=1}^{\infty} v_{0_{mn}} \sin\left(\frac{m\pi x}{a}\right) \cos\left(\frac{n\pi y}{b}\right) & v_0^* &= \sum_{m=1}^{\infty}\sum_{n=1}^{\infty} v_{0_{mn}}^* \sin\left(\frac{m\pi x}{a}\right) \cos\left(\frac{n\pi y}{b}\right)\\
w_0 &= \sum_{m=1}^{\infty}\sum_{n=1}^{\infty} w_{0_{mn}} \sin\left(\frac{m\pi x}{a}\right) \sin\left(\frac{n\pi y}{b}\right) & w_0^* &= \sum_{m=1}^{\infty}\sum_{n=1}^{\infty} w_{0_{mn}}^* \sin\left(\frac{m\pi x}{a}\right) \sin\left(\frac{n\pi y}{b}\right)\\
\theta_x &= \sum_{m=1}^{\infty}\sum_{n=1}^{\infty} \theta_{x_{mn}} \cos\left(\frac{m\pi x}{a}\right) \sin\left(\frac{n\pi y}{b}\right) & \theta_x^* &= \sum_{m=1}^{\infty}\sum_{n=1}^{\infty} \theta_{xmn}{}^* \cos\left(\frac{m\pi x}{a}\right) \sin\left(\frac{n\pi y}{b}\right)\\
\theta_y &= \sum_{m=1}^{\infty}\sum_{n=1}^{\infty} \theta_{y_{mn}} \sin\left(\frac{m\pi x}{a}\right) \cos\left(\frac{n\pi y}{b}\right) & \theta_y^* &= \sum_{m=1}^{\infty}\sum_{n=1}^{\infty} \theta_{y_{mn}}^* \sin\left(\frac{m\pi x}{a}\right) \cos\left(\frac{n\pi y}{b}\right)\\
\theta_z &= \sum_{m=1}^{\infty}\sum_{n=1}^{\infty} \theta_{z_{mn}} \sin\left(\frac{m\pi x}{a}\right) \sin(\frac{n\pi y}{b}) & \theta_z^* &= \sum_{m=1}^{\infty}\sum_{n=1}^{\infty} \theta_{z_{mn}}^* \sin\left(\frac{m\pi x}{a}\right) \sin\left(\frac{n\pi y}{b}\right)\\
q_z^+ &= \sum_{m=1}^{\infty}\sum_{n=1}^{\infty} q_{z_{mn}}^+ \sin\left(\frac{m\pi x}{a}\right) \sin\left(\frac{n\pi y}{b}\right) & \xi(x,z) &= \sum_{m=1}^{\infty}\sum_{n=1}^{\infty} \xi_{mn}(z) \sin\left(\frac{m\pi x}{a}\right) \sin\left(\frac{n\pi y}{b}\right)
\end{aligned} \tag{14}$$

where q_z^+ is the mechanical loading term and $\xi(x, z)$ is the electrical loading term. Through thickness electric potential $\xi_{mn}(z)$ is assumed as per the following.

The elastic FG layer is attached with distributed actuator layer of PFRC. The thickness of the PFRC layer is small as compared to the thickness of the substrate, the electro-static potential in the actuator layer is assumed to be linear through the thickness of the PFRC layer.

$$\xi_{mn}(z) = \left(\frac{V_{mn}^t}{t_p}\right) z - \left(\frac{V_{mn}^t h}{2t_p}\right) \tag{15}$$

Equation 15 gives linear variation of thought thickness electro-static potential in the PFRC actuating layer. V_{mn}^t represents amplitude of doubly sinusoidal electrostatic potential applied at top of the PFRC whereas; h and t_p are thicknesses of elastic FG plate and PFRC layer, respectively. Assumed electrostatic potential satisfies zero electric potential at interface. Similar electrostatic potential can be assumed for PFRC layer at bottom of FG plate.

The piezoelectric stress vectors are calculated from second set of Eq. 6 by substituting actuating electric function (Eq. 15) when either top or bottom voltages (V_{mn}^t, V_{mn}^b) are applied. Finally, piezoelectric stress resultants are evaluated from Eq. 10. Similarly elastic stress vectors and elastic stress resultants are calculated from first set of Eqs. 6 and 9, respectively. Displacement terms are obtained by solving linear algebraic equations by substituting total stress resultants from Eq. 11 in a set of equilibrium equations (Eq. 12).

3 Numerical results and discussions

Numerical evaluation of a FG plate attached with piezoelectric layer either at top or at bottom is considered. Property of piezoelectric fiber reinforced composite is taken as follows (Ray and Sachade 2006b).

FG Material: $E_0 = 200$ GPa and $v = 0.3$.

PFRC (PZT5H): $C_{11} = 32.6$ GPa, $C_{11} = 4.3$ GPa, $C_{22} = 7.2$ GPa, $C_{44} = 1.05$ GPa, $C_{55} = C_{44} = 1.29$ GPa, $e_{31} = -6.76$ C/m^2, $e_{32} = e_{15} = e_{24} = e_{33} = 0.000$, $\varepsilon_{11} = \varepsilon_{22} = 0.037 \times 10^{-9}$ F/m^2, $\varepsilon_{33} = 10.64 \times 10^{-9}$ F/m^2.

Results for displacements and stresses are obtained for following cases.

Case I: $E_h/E_0 = 10$, $q^+_{z_{mn}} = -40$ N/m^2, $V^t_{mn} = 0$, 100, -100, S = 10, 20, 100, PFRC at top

Case II: $E_h/E_0 = 0.1$, $q^+_{z_{mn}} = -40$ N/m^2, $V^t_{mn} = 0$, 100, -100, S = 10, 20, 100, PFRC at top

Case III: $E_h/E_0 = 10$, $q^+_{z_{mn}} = -40$ N/m^2, $V^b_{mn} = 0$, 100, -100, S = 10, 20, 100, PFRC at bottom

Case IV: $E_h/E_0 = 0.1$, $q^+_{z_{mn}} = -40$ N/m^2, $V^b_{mn} = 0$, 100, -100, S = 10, 20, 100, PFRC at bottom.

Where E_h is Young's modulus at top of FG plate.

Results are compared with 3D exact solution (Ray and Sachade 2006a) and FE solutions (Ray and Sachade 2006b). In-plane displacement, transverse

Table 1 FG plates ($\mathbf{E_h/E_0} = 0.1$) with applied sinusoidal mechanical and electrical loadings | PFRC at top

Aspect ratio		S = 10			S = 20			S = 100		
Quantity	Source	$V = 0$	$V = 100$	$V = -100$	$V = 0$	$V = 100$	$V = -100$	$V = 0$	$V = 100$	$V = -100$
$\bar{w}$	Present[a]	−8.6140	3164.12	−3181.35	−8.3577	790.3310	−807.046	−8.2750	23.7481	−40.2981
	3D[b]	−8.7397	3253.30	−3270.80	−8.5437	813.7105	−830.7979	−8.4806	23.9160	−40.5745
	FEM[c]	−8.6673	3212.90	−3230.30	−8.4154	797.9455	−814.7764	−8.3292	24.4974	−41.4587
$\bar{u}$	Present[a]	−0.0905	−3.8486	3.6674	−0.0899	−1.14816	0.988288	−0.089722	−0.1336	−0.04584
		0.1653	−112.9800	113.311	0.1689	−26.5921	26.9299	0.170091	−0.8807	1.22091
	3D[b]	−0.0914	−3.1845	3.0017	−0.0912	−0.9839	0.8015	−0.0912	−0.1285	−0.0539
		0.1686	−114.0117	114.3489	0.1735	−27.0971	27.4441	0.175	−0.8991	1.2493
	FEM[c]	−0.0901	−3.0418	2.8616	−0.0902	−1.0641	0.8838	−0.0901	−0.1322	−0.0480
		0.1714	−107.7880	108.1308	0.1716	−26.3653	26.7085	0.1715	−0.8840	1.2270
$\bar{\sigma}_x$	Present[a]	0.3908	−33.732	34.5138	0.3848	−7.74463	8.57438	0.38294	0.06279	0.703096
		−0.0848	47.3070	−47.4767	−0.0846	11.26	−11.4293	−0.0845	0.3627	−0.53194
	3D[b]	0.4042	−41.0915	41.8999	0.4031	−9.8557	10.6619	0.4027	−0.0061	0.8115
		−0.0807	44.3075	−44.4689	−0.0796	10.6491	−10.8083	−0.0793	0.3451	−0.5036
	FEM[c]	0.4066	−42.1225	42.9357	0.4068	−9.6579	10.4715	0.4066	0.0199	0.8013
		−0.0793	43.0275	−43.1862	−0.0794	10.5905	−10.7493	−0.0793	0.3460	−0.5046
$\bar{\sigma}_y$	Present[a]	0.3763	−163.0770	163.83	0.3697	−41.0169	41.7565	0.36762	−1.29497	2.03021
		−0.0866	30.8163	−30.9899	−0.0862	7.70831	−7.88081	−0.08611	0.22666	−0.398894
	3D[b]	0.3900	−170.3199	171.0999	0.3883	−43.1562	43.9327	0.3877	−1.3654	2.1408
		−0.0825	28.1032	−28.2681	−0.0812	7.1105	−7.2729	−0.0808	0.2088	−0.3704
	FEM[c]	0.3916	−172.9020	173.6851	0.3913	−43.5671	44.3496	0.3909	−1.3748	2.1565
		−0.0810	28.0609	−28.2229	−0.0810	7.0834	−7.2453	−0.0809	0.2072	−0.3689
$\bar{\tau}_{xy}$	Present[a]	−0.2116	55.3721	−55.7955	−0.20979	13.8615	−14.2811	−0.2091	0.356017	−0.77434
		0.0408	−19.0577	19.1394	0.04162	−4.6504	4.7336	0.0418	−0.144775	0.228522
	3D[b]	−0.2138	56.9184	−57.3461	−0.2131	14.2724	−14.6986	−0.2128	0.3692	−0.7948
		0.0416	−19.4500	19.5333	0.0427	−4.7790	4.8645	0.0431	−0.1491	0.2353
	FEM[c]	−0.2148	57.9332	−58.3627	−0.2148	14.3377	−14.7673	−0.2147	0.3667	−0.7962
		0.0431	−19.1536	19.2399	0.0431	−4.7614	4.8477	0.0431	−0.1489	0.2352

[a] Present-HOSNT12 using linear variation of electrostatic potential through the thickness

[b] 3D-Exact (Ray and Sachade 2006a)

[c] FEM-FOST based (Ray and Sachade 2006b)

Table 2 FG plates ($\mathbf{E_h/E_0} = 10$) with applied sinusoidal mechanical and electrical loadings | PFRC at top

Aspect ratio		S = 10			S = 20			S = 100		
Quantity	Source	$V = 0$	$V = 100$	$V = -100$	$V = 0$	$V = 100$	$V = -100$	$V = 0$	$V = 100$	$V = -100$
$\bar{w}$	Present[a]	−0.9575	187.8140	−189.7290	−0.925107	45.5336	−47.3839	−0.914657	0.934162	−2.76348
	3D[b]	−0.9553	186.8222	−188.7329	−0.9252	45.5393	−47.3897	−0.9155	0.9368	−2.7678
	FEM[c]	−0.9485	183.9178	−185.8148	−0.9233	45.2938	−47.1403	−0.9145	0.9328	−2.7619
$\bar{u}$	Present[a]	−0.0194	−0.02330	−0.0155778	−0.0194653	−0.0340133	−0.0049172	−0.019472	−0.0202358	−0.0187082
		0.00929	−5.98321	6.0018	0.00925981	−1.46852	1.48704	0.00924851	−0.0496006	0.0680976
	3D[b]	−0.0194	−0.0307	−0.0081	−0.00195	−0.0337	−0.0053	−0.0195	−0.0202	−0.0188
		0.0093	−5.9373	5.9558	0.0093	−1.4670	1.4855	0.0093	−0.0497	0.0682
	FEM[c]	−0.0195	0.0459	−0.0849	−0.0195	−0.0297	−0.0093	−0.0195	−0.0202	−0.0187
		0.0093	−5.9402	5.9588	0.0093	−1.4655	1.4840	0.0093	−0.0496	0.0681
$\bar{\sigma}_x$	Present[a]	0.0873	−5.91425	6.08905	0.0872538	−1.36822	1.54273	0.0871992	0.0295867	0.144812
		−0.424694	206.348	−207.1980	−0.41905	50.5808	−51.4189	−0.417243	1.6138	−2.44829
	3D[b]	0.0871	−5.8052	5.9794	0.0873	−1.3742	1.5489	0.0874	0.0291	0.1457
		−0.4201	203.984	−204.8249	−0.4171	50.3911	−51.2253	−0.4161	1.6124	−2.4446
	FEM[c]	0.0893	−6.1985	6.3772	0.0893	−1.4170	1.54273	0.0893	0.0299	0.1486
		−0.4250	208.1964	−209.0447	−0.4250	51.4183	−51.4189	−0.4247	1.6447	−2.4941
$\bar{\sigma}_y$	Present[a]	0.0873	−19.8310	20.0051	0.0871659	−4.92925	5.10358	0.0871125	−0.11401	0.288235
		−0.4256	59.2543	−60.1056	−0.419945	14.4701	−15.3100	−0.418129	0.177088	−1.01335
	3D[b]	0.0870	−19.6720	19.8460	0.0872	−4.9333	5.1078	0.0873	−0.1145	0.2892
		−0.4213	57.9752	−58.8178	−0.4180	14.3338	−15.1698	−0.4170	0.1751	−1.0090
	FEM[c]	0.0893	−20.1638	20.3424	0.0893	−5.0400	5.2185	0.0892	−0.1167	0.2951
		−0.4260	58.2432	−59.0951	−0.4259	14.5560	−15.4079	−0.4256	0.1772	−1.0283
$\bar{\tau}_{xy}$	Present[a]	−0.0469	6.90208	−6.99595	−0.0469959	1.6983	−1.79231	−0.0470128	0.0228962	−0.116922
		0.2251	−71.0439	71.4941	0.224223	−17.4332	17.8816	0.223943	−0.480296	0.9281183
	3D[b]	−0.0469	6.8593	−6.9530	−0.0470	1.6982	−1.7922	−0.0470	0.0230	−0.1171
		0.2242	−70.4771	70.9256	0.2243	−17.4232	17.8717	0.2243	−0.4813	0.9298
	FEM[c]	−0.0481	7.1027	−7.1989	−0.0481	1.7394	−1.8356	−0.0480	0.0233	−0.1194
		0.2290	−71.7882	72.2462	0.2290	−17.7746	18.2326	0.2289	−0.4907	0.9486

[a] Present-HOSNT12 using linear variation of electrostatic potential through the thickness

[b] 3D-Exact (Ray and Sachade 2006a)

[c] FEM-FOST based (Ray and Sachade 2006b)

Table 3 FG plates ($\mathbf{E}_h/\mathbf{E}_0 = 0.1$) with applied sinusoidal mechanical and electrical loadings | PFRC at bottom

Aspect ratio		S = 10			S = 20			S = 100		
Quantity	Source	$V = 0$	$V = 100$	$V = -100$	$V = 0$	$V = 100$	$V = -100$	$V = 0$	$V = 100$	$V = -100$
$\bar{w}$	Present[a]	−9.19787	1776.21	−1794.6	−8.9792	430.705	−448.663	−8.9093	8.59293	−26.4115
	3D[b]	−9.2748	1748.2	−1807.5	−9.0549	436.0142	−454.1240	−8.9338	8.7587	−26.7281
	FEM[c]	−9.2761	1789.0	−1766.7	−9.0233	430.4678	−448.5145	−8.9364	8.6323	−26.5051
$\bar{u}$	Present[a]	−0.0877378	57.1545	−57.3300	−0.0873524	14.0393	−14.2140	−0.0872253	0.475472	−0.649922
		0.187776	0.782843	−0.407292	0.19134	0.470687	−0.0880069	0.192523	0.205344	0.179708
	3D[b]	−0.0890	57.1020	−57.2801	−0.0886	14.1124	−14.2896	−0.0885	0.4783	−0.6552
		0.1890	0.5288	−0.1507	0.1925	0.3882	−0.0032	0.1936	0.2029	0.1844
	FEM[c]	−0.0877	57.1020	−57.0792	−0.0878	14.0431	−14.2186	−0.0877	0.4760	−0.6514
		0.1931	−0.0201	0.4063	0.1932	0.3963	−0.0100	0.1930	0.2046	0.1815
$\bar{\sigma}_x$	Present[a]	0.412244	−200.266	201.091	0.410056	−49.1317	49.9519	0.409351	−1.5643	2.3830
		−0.0869931	5.11511	−5.28909	−0.0853276	1.17396	−1.34462	−0.0848174	−0.0349471	−0.134688
	3D[b]	0.4032	−195.9356	196.7419	0.4011	−48.4127	49.2150	0.4005	−1.5486	2.3495
		−0.0882	5.4977	−5.6753	−0.0871	1.2984	−1.4726	−0.0866	−0.0313	−0.1419
	FEM[c]	0.4060	−198.9894	199.8015	0.4061	−49.1587	49.9708	0.4058	−1.5729	2.3844
		−0.0882	5.7883	−5.9647	−0.0882	1.3181	−1.4945	−0.0881	−0.0328	−0.1435
$\bar{\sigma}_y$	Present[a]	0.420911	−58.3826	59.2244	0.418502	−14.2690	15.1060	0.417729	−0.169709	1.00517
		−0.086172	18.5407	−18.7130	−0.084498	4.61233	−4.78132	−0.0839818	0.104439	−0.272403
	3D[b]	0.4115	−54.9286	55.7515	0.4093	−13.5769	14.3954	0.4085	−0.1529	0.9700
		−0.0880	18.8895	−19.0655	−0.0863	4.7369	−4.9096	−0.0858	0.1082	−0.2798
	FEM[c]	0.4148	−54.2976	55.1272	0.4147	−13.5690	14.3984	0.4143	−0.1484	0.9771
		−0.0874	19.2664	−19.4412	−0.0874	4.8161	−4.9909	−0.0873	0.1096	−0.2842
$\bar{\tau}_{xy}$	Present[a]	−0.216361	67.1785	−67.6112	−0.215319	16.4960	−16.9266	−0.214978	0.451734	−0.88169
		0.0449675	−6.52363	6.61356	0.0458246	−1.60544	1.69706	0.0461082	−0.0200694	0.112286
	3D[b]	−0.2193	67.4898	−67.9285	−0.2182	16.6863	−17.1227	−0.2178	0.4581	−0.8937
		0.0453	−6.5681	6.6587	0.0461	−1.6255	1.7177	0.0464	−0.0207	0.1135
	FEM[c]	−0.2208	68.2317	−68.6734	−0.2209	16.8966	−17.3383	−0.2208	0.4635	−0.9051
		0.0472	−6.7491	6.8436	0.0472	−1.6521	1.7466	0.0472	−0.0207	0.1151

[a] Present-HOSNT12 using linear variation of electrostatic potential through the thickness

[b] 3D-Exact (Ray and Sachade 2006a)

[c] FEM-FOST based (Ray and Sachade 2006b)

Table 4 FG plates ($\mathbf{E_h/E_0} = 10$) with applied sinusoidal mechanical and electrical loadings | PFRC at bottom

Aspect ratio		S = 10			S = 20			S = 100		
Quantity	Source	$V = 0$	$V = 100$	$V = -100$	$V = 0$	$V = 100$	$V = -100$	$V = 0$	$V = 100$	$V = -100$
$\bar{w}$	Present[a]	−0.947226	359.141	−361.04	−0.917196	89.2463	−91.0807	−0.906725	2.70149	−4.51494
	3D[b]	−0.9428	359.0874	−360.9938	−0.9164	89.5468	−91.3877	−0.9076	2.7147	−4.5346
	FEM[c]	−0.9416	360.3108	−362.1940	−0.9205	89.4064	−91.2392	−0.9100	2.7028	−4.5180
$\bar{u}$	Present[a]	−0.0190675	12.6577	−12.6960	−0.0191924	2.95976	−2.99815	−0.0192024	0.0974827	−0.135888
		0.00931946	0.268849	−0.250213	0.00928045	0.086099	−0.0675381	0.00926873	0.0125003	0.00603718
	3D[b]	−0.0192	12.4664	−12.5049	−0.0193	2.9557	−2.9942	−0.0193	0.0978	−0.1364
		0.0093	0.2578	−0.2391	0.0093	0.0835	−0.0649	0.0093	0.0124	0.0062
	FEM[c]	−0.0193	11.9237	−11.9622	−0.0193	2.9147	−2.9532	−0.0192	0.0974	−0.1359
		0.0093	0.1967	−0.1781	0.0093	0.0811	−0.0625	0.0093	0.0125	0.0061
$\bar{\sigma}_x$	Present[a]	0.0874028	−50.2609	50.4364	0.0876786	−11.8397	12.015	0.0876465	−0.380849	0.556142
		−0.420162	47.7941	−48.6351	−0.414707	11.1666	−11.9961	−0.412857	0.0440507	−0.569764
	3D[b]	0.0865	−48.6233	48.7963	0.0866	−11.6559	11.8291	0.0866	−0.3775	0.5507
		−0.4228	47.6247	−48.4703	−0.4179	11.4491	−12.2848	−0.4163	0.05640	−0.8890
	FEM[c]	0.0883	−47.8463	48.0230	0.0883	−11.7681	11.9448	0.0883	−0.3842	0.5608
		−0.4250	50.8126	−51.6626	−0.4250	11.7704	−12.6204	−0.4246	0.0546	−0.9039
$\bar{\sigma}_y$	Present[a]	0.0877433	−32.4460	32.6220	0.0878632	−8.04252	8.21825	0.0878223	−0.23732	0.412964
		−0.417512	186.451	−187.289	−0.412987	46.6489	−47.4769	−0.411122	1.47566	−2.2979
	3D[b]	0.0867	−31.3030	31.4763	0.0868	−7.8872	8.0607	0.0868	−0.2338	0.4074
		−0.4212	185.7531	−186.5955	−0.4162	46.9151	−47.7476	−0.4146	1.4889	−2.3181
	FEM[c]	0.0885	−31.8707	32.0478	0.0885	−8.0314	8.2085	0.0885	−0.2378	0.4147
		−0.4233	190.3620	−191.2086	−0.4232	47.8967	−48.7431	−0.4229	1.5168	−2.3626
$\bar{\tau}_{xy}$	Present[a]	−0.046249	21.2813	−21.7741	−0.0464728	5.25403	−5.34698	−0.0464927	0.163813	−0.256798
		0.22389	−62.8314	63.2801	0.223412	−15.6605	16.1073	0.223122	−0.41372	0.859963
	3D[b]	−0.0466	21.4662	−21.5594	−0.0467	5.2583	−5.3516	−0.0467	0.1646	−0.2579
		0.2249	−62.8348	63.2847	0.2240	−15.7140	16.1620	0.2237	−0.4161	0.8634
	FEM[c]	−0.0476	21.4743	−21.5695	−0.0476	5.3330	−5.4282	−0.0476	0.1674	−0.2626
		0.2282	64.9662	65.4226	0.2282	−16.0699	16.5264	0.2282	−0.4228	0.8791

[a] Present-HOSNT12 using linear variation of electrostatic potential through the thickness

[b] 3D-Exact (Ray and Sachade 2006a)

[c] FEM-FOST based (Ray and Sachade 2006b)

displacement, in-plane normal stresses and transverse shear stress are evaluated and their comparison with exact and FEM solutions are presented in Tables and Figures.

Tables 1, 2, 3, and 4 show comparison of numerical results of for the cases I, II, III and IV, respectively.

Figure 2a and b demonstrates normalized variation of transverse displacement ($\bar{w}$) and in-plane displacement ($\bar{u}$) through the thickness of thin FG plate ($S = 100$), respectively. Transverse displacement is constant through the thickness of the FG layer while, in-plane displacement is linear. Normalized variations of in-plane normal stresses ($\bar{\sigma}_x$, $\bar{\sigma}_y$) through the thickness of thin FG plate are exhibited in Fig. 3a and b. Variation of in-plane normal stress ($\bar{\sigma}_x$) at top of FG plate is more than in-plane normal stress ($\bar{\sigma}_y$). This is due to effectiveness of piezoelectric stress coefficient only

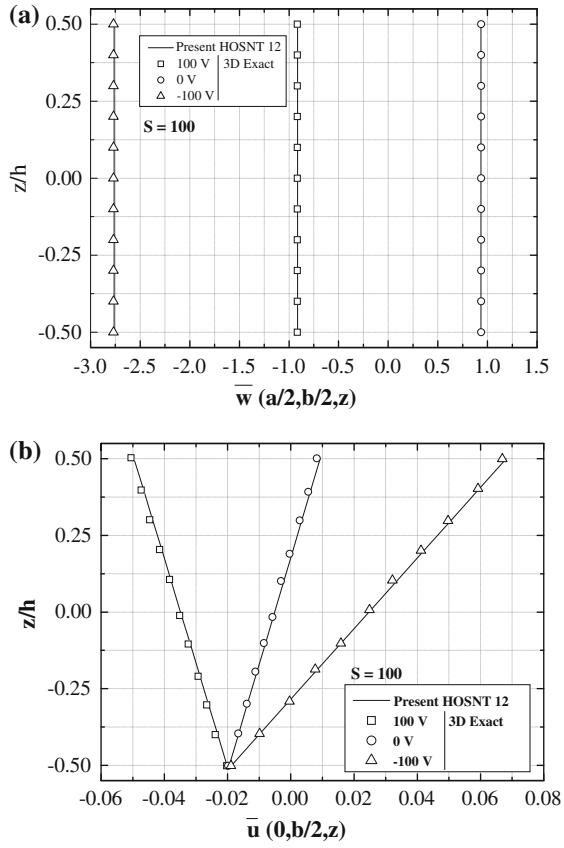

Fig. 2 Variation of normalized (**a**) Transverse displacement $\bar{w}$ (**b**) In-plane displacement $\bar{u}$ through the thickness (z/h) of a Functionally Graded (FG) plate ($E_h/E_0 = 10$) simply supported on all edges with or without applied voltage to the piezoelectric layer

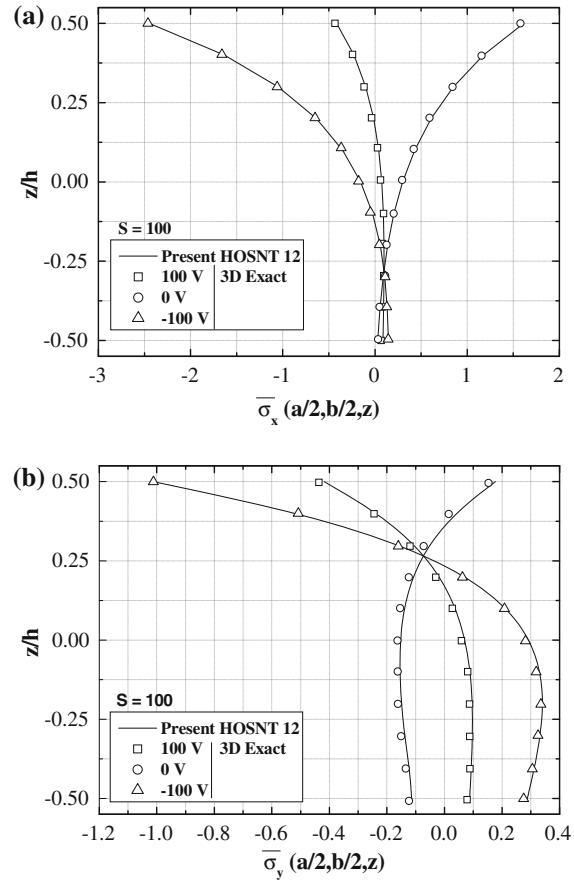

Fig. 3 Variation of normalized (**a**) In-plane normal stress $\bar{\sigma}_x$ (**b**) In-plane normal stress $\bar{\sigma}_y$ through the thickness (z/h) of a Functionally Graded (FG) plate ($E_h/E_0 = 10$) simply supported on all edges with or without applied voltage to the piezoelectric layer

along x-axis. Present HOSNT12 results are closed to exact solution for with or without applied voltages. Figure 4a and b demonstrates normalized variation of in-plane shear stress ($\bar{\tau}_{xy}$) and transverse normal stress ($\bar{\sigma}_z$) through the thickness of thin FG plate. Results of transverse shear stress ($\bar{\tau}_{yz}$, $\bar{\tau}_{xz}$) closely agree with exact results for both the voltages as shown in Fig. 5a and b, respectively. Traction free conditions for transverse shear stress ($\bar{\tau}_{yz}$) can be observed at bottom as well as at top of FG plate, but maximum shear traction is seen at top of FG plate where actuator is placed.

4 Conclusions

In this paper a complete analytical solution for statics of FG plate attached with distributed PFRC actuator

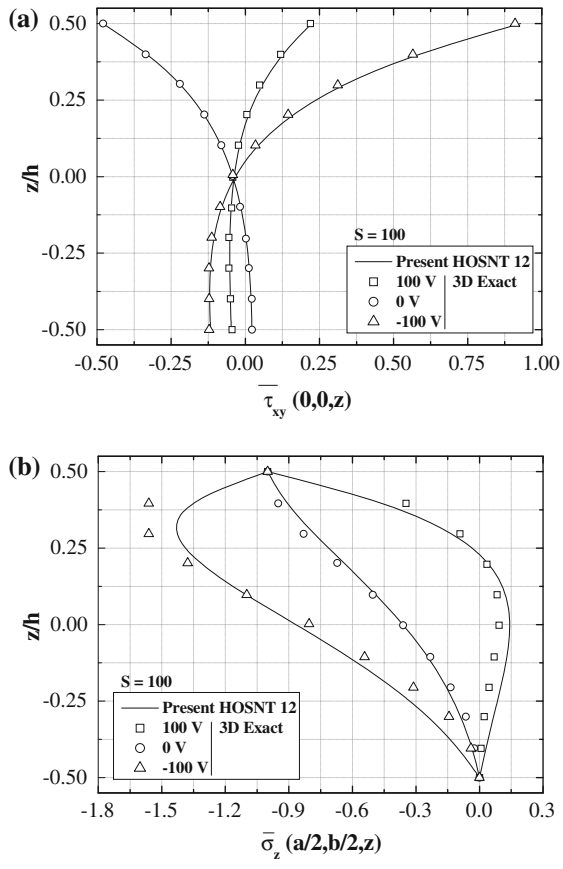

Fig. 4 Variation of normalized (**a**) In-plane shear stress $\bar{\tau}_{xy}$ (**b**) Transverse normal stress $\bar{\sigma}_z$ through the thickness (z/h) of a Functionally Graded (FG) plate $(E_h/E_0 = 10)$ simply supported on all edges with or without applied voltage to the piezoelectric layer

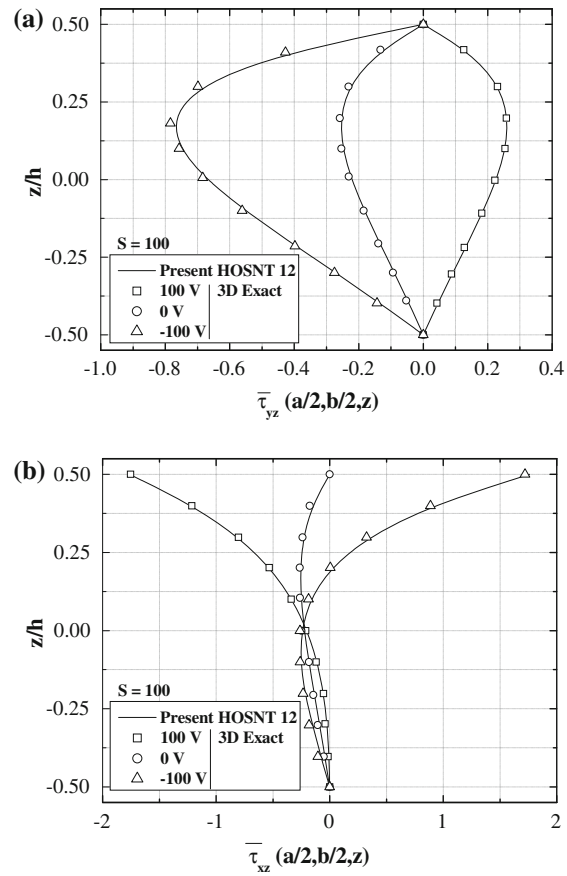

Fig. 5 Variation of normalized (**a**) Transverse shear stress $\bar{\tau}_{yz}$ (**b**) Transverse shear stress $\bar{\tau}_{xz}$ through the thickness (z/h) of a Functionally Graded (FG) plate $(E_h/E_0 = 10)$ simply supported on all edges with or without applied voltage to the piezoelectric layer

under electromechanical load is presented. A higher order shear and normal deformation theory is used to model the elastic responses of FG plate subjected to voltages. Linear layer wise approximation of the electrostatic potential is proposed in the present model. Comparative numerical results and across the thickness variations of displacements and stresses are presented. Linear and constant variations of in-plane and transverse displacements are observed. Considerable effect of actuation at the interface is observed in case of in-plane normal stress and transverse shear stress along x-axis as compared to their effects along y-axis. Present model performs excellently to predict the variations in these cases.

References

Batra, R.C., Vel, S.S.: Exact solution for thermoelastic deformations of functionally graded thick rectangular plates. AIAA J. **40**(7), 1421–1433 (2001)

Heyliger, P.: Static behavior of laminated elastic/piezoelectric plates. AIAA J. **32**, 2481–2484 (1994)

Heyliger, P.: Exact Solutions for simply supported laminated piezoelectric plates. ASME J. Appl. Mech. **64**, 299–306 (1997)

Kant, T.: Numerical analysis of thick plates. Comput. Methods Appl. Mech. Eng. **31**, 1–18 (1982)

Kant, T., Manjunatha, B.S.: An unsymmetric FRC laminate C^o finite element model with 12 degrees of freedom per node. Eng. Comput. **5**(4), 300–308 (1988)

Kant, T., Manjunatha, B.S.: On accurate estimation of transverse stresses in multilayer laminates. Comput. Struct. **50**, 351–365 (1994)

Kant, T., Owen, D., Zinkiewicz, O.C.: A refined higher-order C^o plate bending element. Comput. Struct. **15**, 177–183 (1982)

Kant, T., Swaminathan, K.: Analytical solutions for the static analysis of laminated composite and sandwich plates based on a higher order refined theory. Compos. Struct. **56**, 329–344 (2002)

Kapuria, S., Dumir, P.C.: Coupled FSDT for piezothermoelectric hybrid rectangular plate. Int. J. Solids Struct. **37**, 6131–6153 (2000)

Mallik, N., Ray, M.C.: Effective coefficients of piezoelectric fiber reinforced composites. AIAA J. **41**(4), 704–710 (2003)

Pagano, N.J.: Exact solution for rectangular bidirectional composites and sandwich plates. J. Compos. Mater. **4**, 20–34 (1970)

Pandya, B.N., Kant, T.: A consistent refined theory for flexure of a symmetric laminate. Mech. Res. Commun. **14**, 107–113 (1987)

Pandya, B.N., Kant, T.: A refined higher-order generally orthotropic C^0 plate bending element. Comput. Struct. **28**, 119–133 (1988)

Ray, M.C., Sachade, H.M.: Exact Solutions for the Functionally Graded Plates Integrated With a Layer of Piezoelectric Fiber-Reinforced Composite. ASME J. Appl. Mech. **73**(4), 622–633 (2006a)

Ray, M.C., Sachade, H.M.: Finite element analysis of smart functionally graded plates. Int. J. Solids Struct. **43**, 5468–5484 (2006b)

Ray, M.C., Bhattacharya, R., Samanta, B.: Exact Solutions for static analysis of intelligent structures. AIAA J. **31**, 1684–1691 (1993)

Reddy, J.N.: A simple higher order theory for laminated plates. ASME J. Appl. Mech. **51**, 745–752 (1984)

Reddy, J.N., Cheng, Z.Q.: Three-dimensional solutions of smart functionally graded plates. ASME J. Appl. Mech. **68**(3), 234–241 (2001)

Sankar, B.V.: An elasticity solution for functionally graded beams. Compos. Sci. Tech. **61**(5), 689–696 (2001)

Smith, W.A., Auld, B.A.: Modeling 1–3 composite piezoelectrics: thickness mode oscillations. IEEE Trans. Ultrason. Ferroelectr. Frequency Control **31**(1), 40–47 (1991)

Tiersten, H.F.: Linear Piezoelectric Plate Vibrations. Plenum Press, New York (1969)

Tiersten, H.F., Mindlin, R.D.: Forced vibrations of piezoelectric crystal plates. Quart. Appl. Math. **20**, 107–119 (1962)

Vel, S.S., Batra, R.C.: Three-dimensional analytical solution for hybrid multilayered piezoelectric plates. ASME J. Appl. Mech. **67**, 558–567 (2000)